

# Measuring Wing Profile Drag using an Integrating Wake Rake

Ellen A. Pifer  
epifer@slu.edu

Götz Bramesfeld  
gbramesf@slu.edu

*Saint Louis University  
Saint Louis, MO, 63103*

## Abstract

An integrating wake rake concept is discussed here as very suitable for in-flight profile-drag measurements on gliders. The experimental setup is in essence the same as used with other integrating wake rakes, which uses a series of Pitot tubes that feed into a single manifold to measure the averaged total pressure deficit in the wake of an airfoil. The difference compared to those conventional integrating wake rakes lies in the post-measurement data reduction. In an iterative approach, the measured pressures are corrected in order to account for the unknown shape of the wake-deficit region and other unidentified parameters. With this approach, the possible accuracies in profile drag are similar to those obtained using a traversing wake survey system. Thus, in contrast with conventional wake rakes, it is possible to measure accurate absolute drags of an actual section of a wing in flight that can be compared with previous wind-tunnel results and/or theoretical predictions. The general theory of this drag measurement device is discussed in this paper. Furthermore, the experimental apparatus developed at Saint Louis University is introduced. Preliminary results of a comparison study demonstrate the capability of the system and the approach to measure profile drag during flight.

## Nomenclature

$c$	airfoil chord
$c_d$	section drag coefficient
$D$	tube diameter
$F$	integration factor
$n$	number of tubes of wake rake
$p$	static pressure
$p_t$	total pressure
$q$	dynamic pressure
Re	Reynolds number
$t/c$	thickness ratio
$\alpha$	angle of attack
$\eta$	non-dimensional maximum total pressure deficit in the wake
$\mu$	absolute viscosity
$\rho$	density
$\xi$	distance behind trailing edge
$\zeta_r$	rake height
$\zeta_{wake}$	wake height

## Subscripts

av	average
$i$	inside
$o$	outside
0	freestream conditions
$r$	registered by the integrating wake rake

## Introduction

Drag is a dominant concern in sailplane design as reduced drag translates to improved interthermal cruise performance. Improved interthermal cruise performance leads to an increase in average cross-country speed [1]. In order to assess the performance of the aircraft, accurate drag measurements are needed. This paper introduces a relatively simple method to determine profile drag during flight.

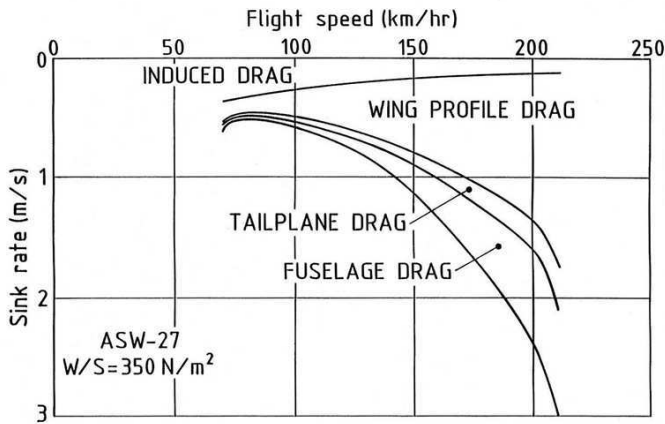
Total drag can be decomposed into several components, the two largest being profile drag and induced drag. Profile drag is primarily a function of the shape and surface quality of the wing section. Induced drag is a result of the production of lift by a wing with finite span and can be related to the downwash that alters the incoming freestream velocity.

Figure 1 depicts the change in sink rate with forward flight speed of a sailplane due to the presence of various drag components. The figure shows that wing profile drag is the major component of drag at higher interthermal flight speeds. The fraction of total drag associated with the induced drag is highest at low velocities. Since there is no thrust generated on a sailplane, it is important to reduce the amount of profile drag to improve the glide performance of the sailplane at cruising velocities. Thus, for a successful, modern, high-performance sailplane design, it is important to assess the impact of geometric section modifications on profile drag correctly, using methods that produce accurate drag measurements.

Profile drag can further be broken up into the combination of pressure drag and skin friction drag. Skin friction drag is primarily due to viscous effects inside the boundary layer near the

---

Revised version of paper presented at the 2012 AIAA Region V Student Conference, Boulder, CO, April 4-6, 2012



**Figure 1** Sink rate contributions of various elements of a typical high-performance sailplane (Courtesy of L.M.M Boermans, TU Delft).

surface of the airfoil. Inside the boundary layer, the flow velocity decreases from free stream conditions to zero at the surface due to the no-slip condition. The subsequent velocity gradient at the surface is directly related to skin friction forces.

Laminar flow has less skin friction than turbulent flow because of its lower velocity gradient at the surface within the boundary layer. In a laminar boundary layer the fluid moves in smooth streamlines parallel to the surface. In a turbulent boundary layer, fluid particles exhibit random flow perturbations in addition to their main flow velocity. Due to the higher degree of mixing, the velocity profile of turbulent flow is “fuller” than that of a laminar boundary layer. This results in steeper velocity gradients at the surface that contribute to higher shear stresses and skin friction drag than laminar boundary layers. These viscous effects within the boundary layer play an important role with respect to flow separation.

Favorable pressure gradients promote the existence of laminar flow and prevent flow separation. Adverse pressure gradients decrease the velocity of the flow along the airfoil and eventually reduce the momentum until it separates from the surface. The plot shown in Fig. 2 depicts the pressure coefficient distribution over the upper surface of an airfoil with the presence of a laminar separation bubble. The constant pressure that is associated with the separation region leads to an increase in pressure drag. In addition, the turbulent boundary layer after reattachment tends to have significantly larger skin friction drag than if transition occurred without separation. Figure 3 depicts the flow conditions inside the laminar separation bubble. Prior to the laminar separation bubble, the boundary layer is dominated by laminar flow and thus low skin friction drag. Around the laminar separation point, the flow under the influence of the adverse pressure gradient detaches from the surface. It can be seen that just after the separation point that the flow is nearly stagnant and even reverses its direction. The lower pressure of the laminar separa-

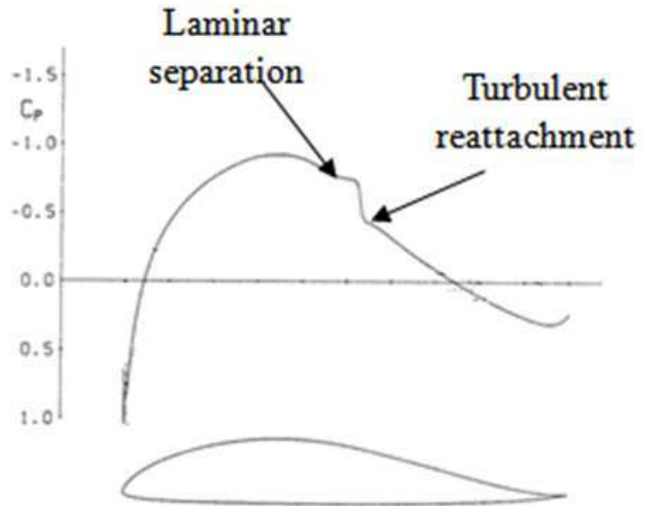


**Figure 2** Pressure coefficient distribution with laminar separation.

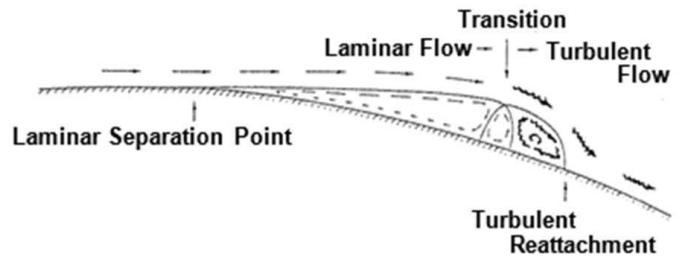


**Figure 3** Flow conditions of a laminar separation bubble [2].

tion bubble results in an increase in pressure drag. Eventually, the outer, detached laminar flow transitions to turbulent flow, thus regaining energy to reattach to the surface.

The challenge for the airfoil designer is to minimize profile drag by extending the laminar flow region as much as possible while avoiding significant flow separation before transition. For typical sailplane airfoils, it is possible to tailor the upper surface pressure distribution in such a way that little or no flow separation occurs and any associated drag penalty is negligible. However, the same treatment is difficult to achieve on the lower surface. Here, the designer uses favorable pressure gradients until a boundary layer tripping device is used to force transition. The subsequent turbulent flow overcomes the adverse pressure gradient to the trailing edge. Without the tripping device, the laminar flow separates. Although the boundary layer trips can prevent laminar separation bubbles, it remains unknown if the additional skin friction drag of the extended turbulent flow is less than the additional drag of the laminar separation bubble.

Forced transition from laminar to turbulent flow before the occurrences of a laminar separation bubble takes advantage of

the higher momentum mixing of the turbulent boundary layer to overcome the adverse pressure gradient. This eliminates the additional pressure drag caused by laminar separation bubbles but increases skin friction drag because of the extended turbulent flow. There are several types of tripping devices or turbulators: zig-zag tape, bump tape, or pneumatic turbulators. One method to assess the changes in profile drag from the introduction of turbulators requires measuring the pressure or momentum loss in the wake. Several methods are currently used in wind tunnels and flight tests to determine the impact of turbulators.

In order to advance the performance of current sailplanes and promote the development of new ones, accurate experimental tools are needed that allow assessing wing sections in flight. The particular interest is to be able to make a judgment about the effectiveness of turbulators. In addition, being able to measure the drag of wing sections on an existing sailplane holds valuable information for the designer. For example, a better understanding of the impact of fabrication related variations on the drag of a wing section provides information about how forgiving or unforgiving a design might be. In addition, the comparison of the drag values of a wing section obtained under free-flight conditions with the values derived using either in wind-tunnel tests or theoretical means, provides the adjustment of those predictive tools for future sailplane developments.

This paper discusses wake survey methods for drag determination with a special emphasis of the use of integrating wake rakes. The theory of an iterative drag estimation is explained that enables drag measurements with accuracies similar to the ones obtained with traversing probes. Such an extended profile drag measurement device was developed at Saint Louis University (SLU) and tested in wind-tunnel tests at The Pennsylvania State University (PSU). The system and its elements are explained. At the end of this paper, experimental results demonstrate the capability of the entire system.

## Wake survey method for profile drag measurements

### General theory

Wake surveys are a common method for measuring profile drag. The wake survey measures static pressures and the decrease in total pressure within the wake and compares those values to the freestream total pressure. This pressure deficit, or essentially the momentum loss of the flow, can then be directly related to the profile drag. An excellent and more complete discussion of how to extract drag from wake pressure deficits can be found in Ref. 3. Nevertheless, a brief review of the general approach is listed in this section.

Figure 4 shows a pictorial representation of the velocities before, station 0, and aft of the airfoil, stations 2 and 1. The shaded area represents the total moment loss and integrating this area gives the profile drag. A wake survey measures drag by collecting pressure readings in the wake and in the freestream; the difference in these pressures translates to the loss of momentum in the flow. The losses are greatest in the center of the

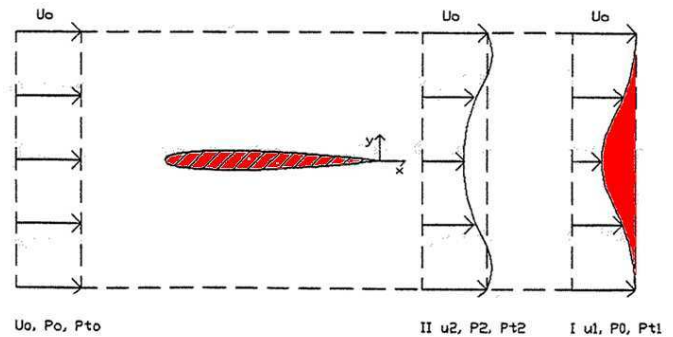


Figure 4 Momentum loss of flow over an Airfoil [3]

wake and decrease moving outward until freestream momentum is achieved as can be seen in Fig. 5. These losses occur because of the boundary layer interaction with the airfoil. While it is difficult to measure the velocities in the wake, Bernoulli's equation provides a relationship between velocity, static pressure, and dynamic pressure.

$$p_t = p + \frac{1}{2}\rho V^2 = p + q \quad (1)$$

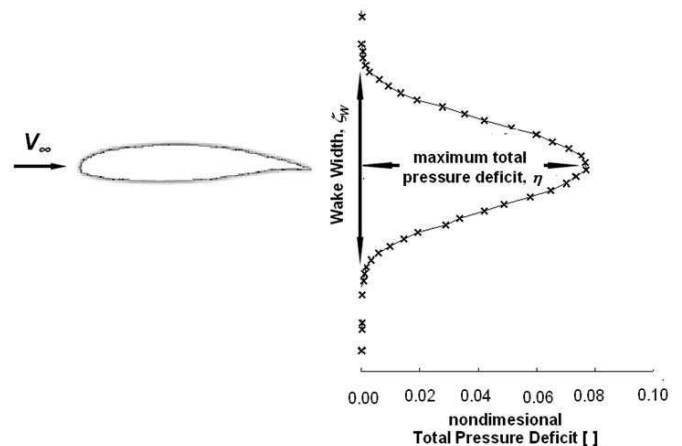
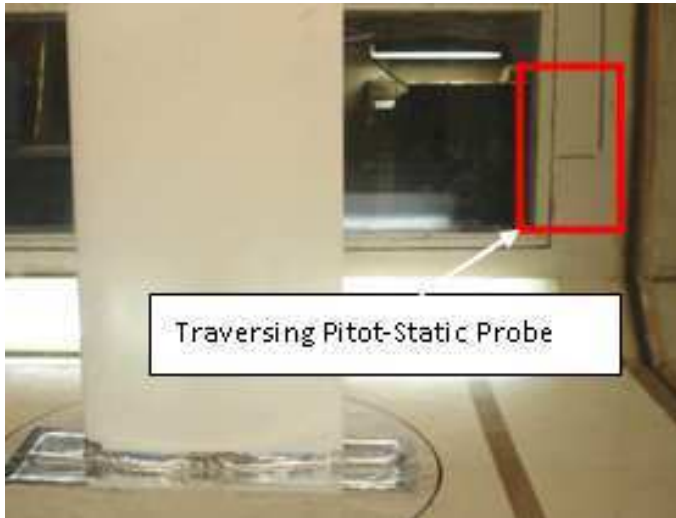


Figure 5 Typical traversing Pitot-static probe and measured pressure deficit in wake.

Using this relationship, the deficit in total pressure,  $p_t$ , within the wake can be related to profile drag of the wing section.

$$c_d \cong \frac{1}{c_{q0}} \int_{\text{wake}} (p_{t0} - p_t) dy \quad (2)$$

The wake pressure deficit has to be measured sufficiently far enough from the trailing edge to allow the static pressure to recover to freestream conditions. Because of the laws of continuity in the freestream flow, static and total pressures are easily measured and may be taken anywhere in the freestream. Further corrections can be applied to adjust for the static pressure in the



**Figure 6** Typical traversing Pitot-static probe as used in wind tunnel tests

wake not having fully recovered at the location of the wake survey [3]. The individual samples of total pressures in the wake,  $p_t$ , can then be integrated across the width of the wake and related to profile drag.

### Wake survey systems

Each type of wake rake operates using the same general theory. The difference is the method used to collect pressure data. In general, three different types of wake surveys are used: conventional wake rake, traversing probe, and integrating wake rake. The conventional wake rake is a series of Pitot probes that span the entire wake and collect pressure data. Individual collections of pressure are accomplished through the use of a manometer, individual pressure transducers or scanivalve. Individual readings within the wake can be accurately measured before they are averaged. An advantage of a conventional wake rake is that it can clearly determine the height and shape of the wake and accurately calculate drag. The disadvantage of this method is the amount of equipment necessary. Separate tubing for each pressure probe and individual pressure transducers or some sort of scanivalve make this method less feasible for in-flight measurements.

In the case of a traversing wake probe, a mechanical actuator moves the wake-survey probe along the width of the wake and enables individual pressure readings at each location. An example is the PSU wake survey system shown in Fig. 6. The readings can be completed in as little as 5–10 seconds depending on the traversing mechanism. An example is of such measurements is given in Fig. 5 The traversing survey system utilizes one pressure transducer, eliminating the need for several pressure transducers, while also maintaining accuracy of the readings. A traversing survey system can also be employed in flight tests [4]. The traversing mechanism, however, adds complexity

and creates the challenge of ensuring constant flight conditions while the probe is surveying the wake. In that case, piloting skills begins to play a large effect in the error of the pressure readings.

### Integrating wake rakes

Integrating wake rakes are much more suitable for flight test applications due to their relative simplicity. An integrating wake rake is similar to the conventional wake survey system except that the individual tubes lead to a single manifold in which the pressures are collected and “pneumatically” averaged. According to Silverstein and Katzoff, under equilibrium conditions, the manifold pressure equals the averages pressures of the sum of the tubes [5]:

$$p_{t_{av}} = \frac{1}{n} \sum_n p_{t_n} \quad (3)$$

Where  $p_{t_{av}}$  is the manifold pressure,  $n$ , the number of rake tubes, and  $p_{t_n}$ , is the total pressure of each tube. A sufficiently large manifold minimizes any internal flows, which, otherwise, can result to measurement errors that depend on free stream velocity and angle of attack.

A similar wake rake design was used by Ref. 6, although this device was attached directly to the trailing edge. That particular rake, however, exhibited rather large errors as a consequence of the large pressure differences between the upper and lower surface flows [7]. Reference 8 uses an integrating wake rake, primarily to detect changes in drag due to the placement of turbulators.

### In-flight wake measurements

In-flight measurements of airfoil drag are of great interest in order to improve the performance of the fabricated wing. Of particular interest is the ability to quantify the influence of turbulators and flap deflections on drag, as well as how well the wing as built duplicates what was previously designed and tested in wind tunnels. The effects of turbulators and flap deflections are primarily changes in drag. The comparison of the actual wing section in flight with previous theoretical or experimental results requires the measurement of absolute drag. Differences may be due to different inflow conditions during free flight or due to shape deviations that result from fabrication or aging factors. Ideally, the designer wants the ability to measure drag during free flight with similar accuracies as achieved in a well-maintained wind tunnel.

For in-flight measurements the integrating wake rake is the preferred tool because of its relatively simplistic design and the minimal instrumentation it requires. Such a wake rake can take data at a single instance in time, whereas in the case of a traversing system, maintaining steady conditions during the duration of the traverse of the wake probe can become challenging. The less complex equipment required for tests using an integrating wake is another significant advantage.



On the other hand, the integrating wake rake provides only very limited accuracy in drag estimation. This is in part due to the fact that the wake rake captures the deficit of the total pressure behind a wing section rather than the momentum deficit, which is related to drag. In order to measure drag accurately, the size and shape of the wake deficit region must be known. Further corrections are needed to account for a static pressure that has not fully recovered to free-stream condition at the location of the wake rake. Although various approaches can be used to account for the static pressure [3], it is very difficult to actually measure the static pressure near the trailing edge of a wing. Another potential error, which leads to an underestimation of the measured drag, is given when the wake rake only partially covers the deficit region of the wake. Increasing the wake rake height in order to ensure the entire pressure deficit region is captured increases the influence of the measured pressure by the unaffected free stream values of the “tails.” The subsequent averaged pressure deficit signal becomes weaker and, therefore, possible errors are introduced due to insufficient resolution of the corresponding pressure transducer. At the center of this paper is an in-flight section-drag measurement device that combines the simplistic design and implementation of a conventional wake rake with the accuracy of a traversing probe system. The actual wake rake is very similar to other integrating wake rakes, such as the one by Ref. 8, that consist of a series of Pitot probes attached to a common manifold. During the post-measurement data reduction, corrections and estimations are applied to the measurements that lead to predicted absolute profile drag values with accuracies very similar to those of a wake survey system. The general workings of such an integrating wake rake and the special data reduction method are discussed in the following sections.

### Principles of the integrating wake rake

Figure 7 shows a picture of the integrating wake rake that was developed at SLU. The wake pressure tubes are located in the middle and are attached to the main manifold while the freestream pressure tubes are located on either end. The two



**Figure 7** Integrating wake rake built at Saint Louis University.

freestream pressure tubes are combined to yield an average total pressure reading from above and below the airfoil. Although the freestream total pressure theoretically is equal, an average of the two freestream pressures helps to eliminate possible errors. Alternatively, the two total pressures can be used as a check if the wake rake covers the entire total pressure deficit region. In any case, the height of this wake rake becomes very important, as both of the outer free stream total pressure tubes must be in the freestream in order to yield good results.

The middle tubes are designed to collect the total pressures of the wake. The tubes feed directly into the main collecting chamber or manifold, from which the averaged pressure of the wake is made available with a single port. The strength of the measured average pressure signal is weakened as more of the wake rake tubes record pressure values of the undisturbed freestream tails. To a certain extent, however, this can be remedied by closing off pressure tubes as needed.

### Drag estimation

Reference 5 considers that the drag acting on an airfoil is proportional to the average total head loss across the wake. Equation 4 shows this relationship:

$$c_d = F \frac{\zeta_r}{c} \frac{p_{t0} - p_{tav}}{q_0} \quad (4)$$

Without knowing the exact shape of the wake as, for example, in Fig. 5 certain corrections must be applied in order to accurately predict profile drag. Reference 5 introduced a correction or integrating factor,  $F$ , that assumes a cosine-square distribution of the pressures across the wake. Wake width,  $\zeta_{wake}$ , and the nondimensional maximum loss of the total pressure in the wake,  $\eta$ , are determined based on empirical relationships that depend on chord Reynolds number and several airfoil characteristics. In wind tunnel experiments, Plaisance [9] showed that using this approach yields good drag prediction results for airfoils with extended laminar flow.

The factor  $F$ , as is shown in Eq. 5, is the integral of the pressures in the wake using estimated wake dimensions and an assumed cosine square shape of the total pressure distribution. The equation also considers the impact of a static pressure that has not yet fully recovered to freestream conditions because of the location of the wake rake relatively close behind the trailing edge. Moving the rake farther back could allow time for the static pressure to recover, but has physical limitations. Applied to the integrating wake rake, Eq. 5 can be integrated numerically fairly simply using the trapezoidal rule.

$$F = \frac{4}{\eta \zeta_{wake}} \int_{wake} \left\{ \left( \sqrt{1 - \frac{p - p_0}{q_0}} - \eta \cos^2 \left( \frac{\pi y}{\zeta_{wake}} \right) \right) \left( 1 - \sqrt{1 - \eta \cos^2 \left( \frac{\pi y}{\zeta_{wake}} \right)} \right) \right\} dy \quad (5)$$

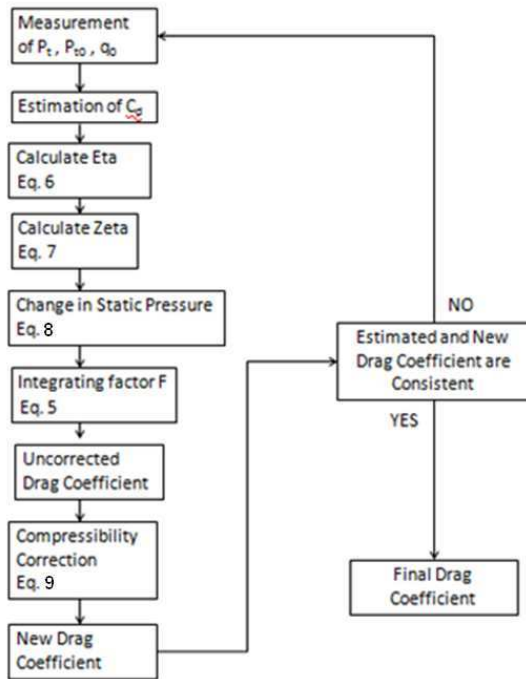


**Figure 8** Flow diagram of data reduction process

The terms  $\eta$  and  $\zeta_{\text{wake}}$  are further functions of the distance from the trailing edge, thickness ratio of the airfoil, and the chord Reynolds number. These functions help to determine the overall shape of the wake and maximum pressure deficit. Plaisance developed empirical relations for  $\eta$  and  $\zeta_{\text{wake}}$ , as shown in Eqs. 6 and 7, for laminar airfoils [9].

$$\eta = (-1.08 \cdot 10^{-12} \text{Re}^2 + 3.35 \cdot 10^{-6} \text{Re} + 4.15) \frac{\sqrt{c_d} \sqrt{t/c}}{\xi + 0.3} \quad (6)$$

$$\frac{\zeta_{\text{wake}}}{c} = (0.34 \cdot 10^{-12} \text{Re}^2 - 1.07 \cdot 10^{-6} \text{Re} + 3.21) \sqrt{c_d} \sqrt{t/c} \sqrt{\xi + 0.15} \quad (7)$$

Since the rake is located a relatively short distance (approximately  $0.2c$  away from the trailing edge), Silverstein and Katzoff derived an empirical equation for the change in static pressure in the wake behind an airfoil [5]. Plaisance extended Silverstein's expression for static pressure differences between freestream and wake with an expression that also captures effects due to changing chord Reynolds numbers [9].

$$\frac{p - p_0}{q_0} = (-1.33 \cdot 10^{-6} \text{Re} + 4.36) \frac{t/c}{(.77 + 3.1\xi)^2} \quad (8)$$

A final correction for compressibility is applied. This correction is added into the previously calculated drag coefficient in

order to calculate the corrected drag coefficient.

$$c_d = c_{d_{\text{incomp}}} \left\{ 1 + \frac{M^2}{8} \left[ 3 \frac{p - p_0}{q_0} + 1 - 2\gamma + 2\eta \cos^2 \left( \frac{\pi y}{\zeta_{\text{wake}}} \right) - (2\gamma - 1) \sqrt{1 - \eta \cos^2 \left( \frac{\pi y}{\zeta_{\text{wake}}} \right)} \right] \right\} \quad (9)$$

It should be noted that the wake width and maximum pressure deficit estimate in Eqs. 6 and 7, respectively, require the profile drag coefficient. Therefore, an iterative process is employed to compute the profile drag coefficient based on an initial guess for the profile drag and is summarized in Fig. 8. The iterative process refines the integration of the momentum loss until the criteria for convergence is met for the change in drag coefficient.

## Integrating wake rake implementation

### Wake rake design and manufacturing process

A wake rake was constructed at SLU and is shown in Fig. 9. The height of the rake is 8 inches (203 mm) so as to fully capture the wake and provide more versatility for its future use on different aircraft sizes and in wind tunnels. For significantly smaller wakes, some of the outer tubes can be blocked off. Pressure tube sizing was determined from past reports with an outer diameter of 1/16 inch (1.6 mm) and an inner diameter of 1/20 inch (1.3 mm) [9]. A total of 64 tubes were used with a spacing of 1/16 inch (1.6 mm) between each tube. Each tube was 3 inches (76 mm) long so as to reduce interference and disturbances to the flow caused by the main pressure collection chamber. Additionally, two pressure tubes were placed at either end of the 8 inch (203 mm) main pressure collection chamber, closer to the free-stream, so as to record total pressure readings. These outermost pressure tubes are directly connected to the pressure transducer using vinyl tubing. The 64 wake pressure tubes are connected to the main collection chamber that has a single port for measuring the average pressure in the wake.

Materials for construction of the wake rake were chosen for their overall strength and stiffness, weight, corrosion, brazing requirements, and cost. Stainless steel was chosen for its high strength to weight ratio. It provided the required rigidity to withstand stresses experienced during flight, will not corrode, and was recommended for its ease of brazing.

An example of how the rake is mounted is shown in Fig. 9. Reference 5 suggests that the wake rake is located approximately  $0.2$  airfoil chord lengths behind the trailing edge in order to yield the best results. Based on the wing chord typical for modern sailplanes, a distance of 7 inches (178 mm) appears desirable [9]. To maintain this distance, a supporting apparatus similar to that in Fig. 9 attaches to the wing. The wake rake is then fastened to the horizontal bar of the apparatus via a simple screw and nut connection. Five different slots allow the user



**Figure 9** Integrating wake rake and its mounting behind wing.

the option of varying the height if necessary for specific testing needs.

The wake rake needs the flexibility to adjust to different heights and angles in order to capture the wake at different angles of attack. Each hole secures the wake rake with a screw and nut connection. The horizontal bar has the ability to rotate and lock to allow the wake rake to operate at different angles.

### Data acquisition and reduction

For the data reduction process it was decided to use a similar code as in [9], which incorporates the drag coefficient and correction factor calculations discussed previously. A Matlab program reduces the pressure data to drag coefficients. The data reduction procedure is integrated in a LabVIEW program that also manages the data acquisition and provides a user-friendly interface. The sensor signals are preconditioned before being reduced in order to minimize the amount of error from electrical noise. As part of the current data reduction setup, the convergence criteria of the iteration as indicated in Fig. 8 is a drag coefficient change of less than 0.00001.

### Sensor integration

There are three separate pressure readings that are fed into the data acquisition program. The hardware set up is shown in Fig. 10. The freestream total pressure is measured with a Kiel

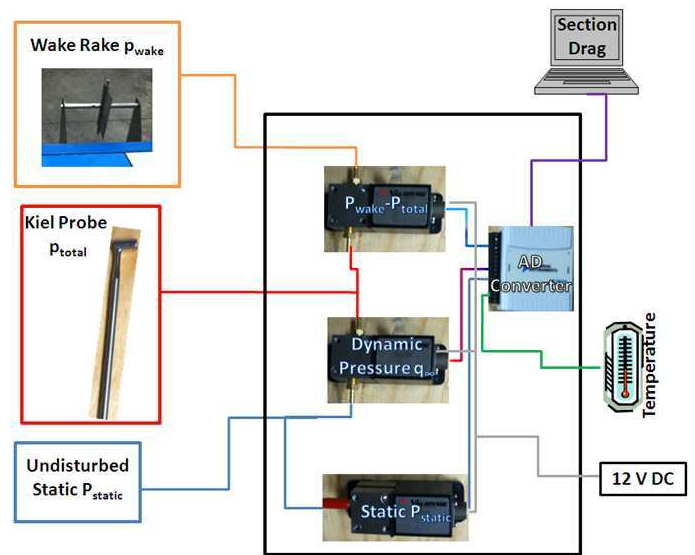


**Figure 10** Instrumentation setup of integrating wake rake.

probe, the average total pressure in the wake is measured with the wake rake and the freestream temperature is measured with a thermocouple. Measuring the freestream static pressure is more involving since the presence of the wing and aircraft causes a perturbation of this value. Thus, for flight tests, either the aircraft static system will be used (which has its own inherent error) or a trailing probe will be employed.

## Wind tunnel, model, and preliminary data

### The PSU low speed wind tunnel and model

To calibrate and validate the wake rake and to refine the integration factor,  $F$ , drag measurements were performed on a two-dimensional airfoil model in the PSU low-speed, low-turbulence wind tunnel. The SLU integrating wake rake and the PSU wake survey system were compared side by side at Reynolds numbers typical to the ones expected in flight tests with sailplanes.

The PSU low-speed, low-turbulence wind tunnel facility is a closed-throat, single return, atmospheric facility. The test section is 3.3 ft high x 4.8 ft wide with filleted, rectangular corners. The maximum attainable test section speed is 220 ft/s. As shown in Fig. 11, an S406 airfoil model that was used in the tests was mounted vertically in the test section and attached to computer-controlled turntables that allow the angle of attack to be set. The wake rake was attached and aligned with the bisector of the flow coming off the trailing edge.

The flow quality of the PSU wind tunnel has been measured and documented [10]. At a velocity of 150 ft/s, the flow angularity is below  $\pm 0.25$  degrees throughout the test section. At this velocity, the mean velocity variation in the test section is below  $\pm 0.2\%$ , and the turbulence intensity is less than 0.045%. The PSU tunnel measurements made on the laminar-flow S805 wind-turbine airfoil [11] are compared with those obtained using the



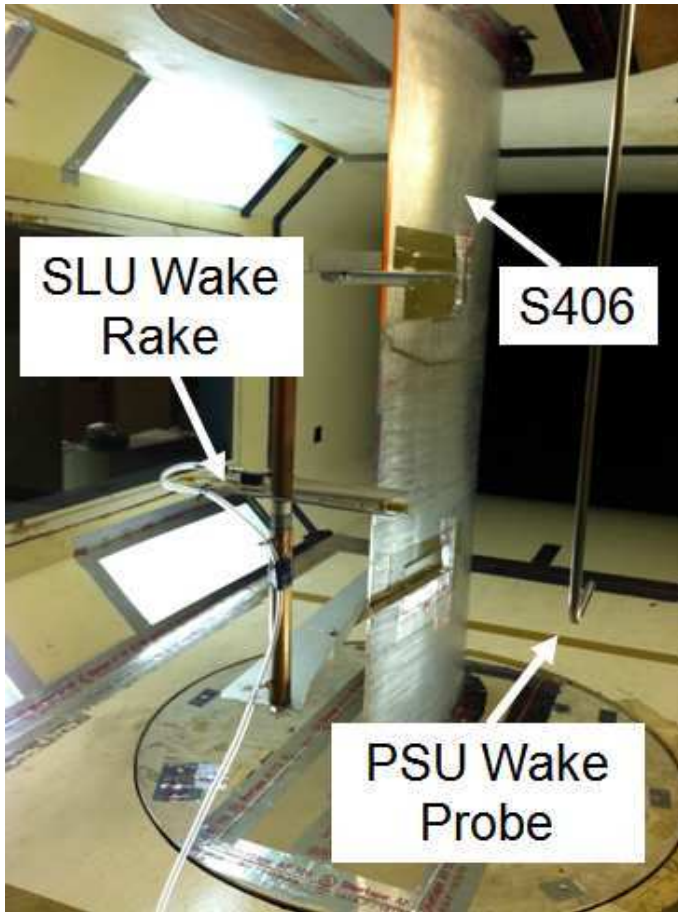


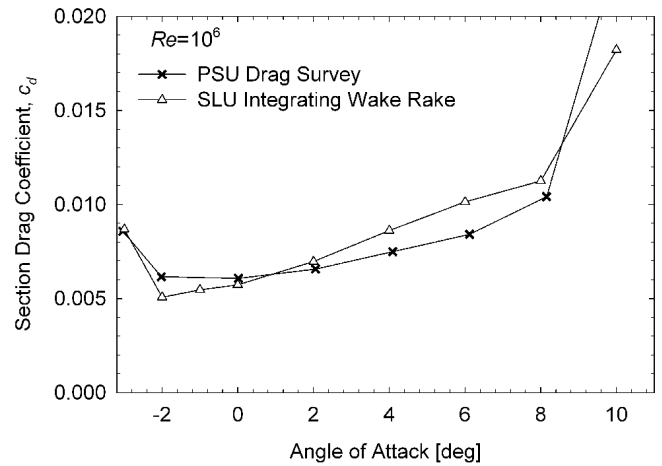
**Figure 11** Setup for tests in PSU low-speed, low turbulence wind tunnel.

same wind-tunnel model at Delft University of Technology [12]. These data demonstrate excellent agreement.

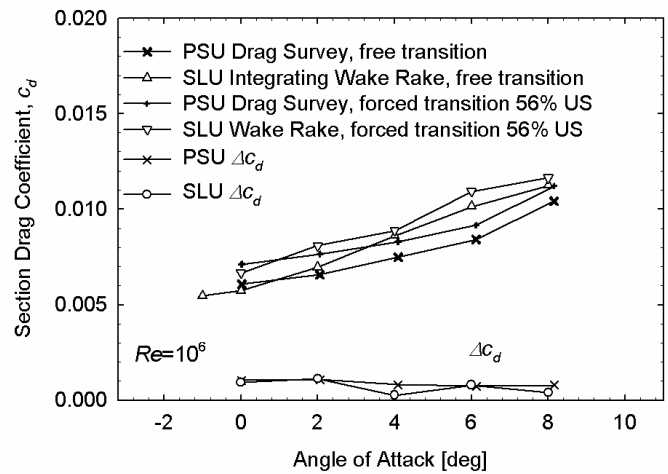
### Preliminary data

Figure 12 shows the total drag measured at a Reynolds number of 1,000,000 comparing drag measurements of the PSU wake survey systems with those of the integrating wake rake using different integration factor constants. After correcting several inconsistencies in the data reduction described by Ref. 9, it was possible to reproduce the results presented therein. In addition, the subsequent results that are shown in Fig. 12 show reasonable agreement between the drag values evaluated using the PSU drag survey system and the SLU integrating wake rake with the iterative approach discussed herein.

A test was also performed to analyze the sensitivity of the wake rake and the ability to measure small changes in drag due to the introduction of a turbulator. As shown in Fig. 13, the clean airfoil drag was measured using both the PSU wake survey and SLU integrating wake rake and then again after introducing the zig-zag tape located at 56% of the chord on the upper surface. The differences between the clean and the zig-zag runs are com-



**Figure 12** Comparison of drag measurements of traversing probe system (PSU) and integrating wake rake.



**Figure 13** Comparison of drag differences due to turbulator measured using traversing probe system (PSU) and integrating wake rake (SLU).

pared between the PSU wake survey system and SLU integrating wake rake. Across most of the low drag region of the airfoil the integrating wake rake is very sensitive to small changes in drags and agree well with the PSU drag surveys.

These results demonstrate the ability of the wake rake to measure the impact of turbulators accurately but also of absolute drag. A more complete discussion of the experiment and the subsequent data will be presented in a future paper.

### Error analysis

During testing at PSU, it became obvious that a more effective method for adjusting gains and offsets of the pressure transducers is needed for the experimental setup of the integrating wake rake. The accuracy of the experimental results is greatly influenced by the sensitivity of the pressure transducer that records



the relatively small magnitudes of the averaged total pressure deficits of the wake of only a few pascals. During the tests, recording wind-off values of the pressure transducers and subtracting those values from subsequent data points resulted in significantly different drag results. Overall, the calculation of the drag coefficients was found to be extremely sensitive to very small changes in pressures. Therefore, further modifications to the data acquisition and reduction program are implemented in order to condition the signals. The proper setup of the instrumentation will be performed before further wind tunnel tests are performed. Furthermore, a pressure transducer with a smaller pressure range is under consideration to increase the sensitivity of the pressure readings, especially of the averaged total pressure deficits measured by the wake rake.

### Conclusions

Preliminary testing has shown that more analysis must be completed before the integrating wake rake can measure absolute drag. Proper signal conditioning will help to greatly improve the accuracy of the measurements and more wind tunnel testing is needed to decide on an integrating factor. The wake rake is a very sensitive tool, as was seen when comparing the delta drags between the clean airfoil and the use of zig-zag tape. This is a very promising result as it will help assess the increase or decrease in profile drag caused by turbulators.

Building and assembling a functioning wake-rake system for flight testing and further adjustments to the program to add signal filtering are currently in process. Once the system is set up, further validation and calibration of the system in Saint Louis University's wind tunnel will be performed. Further data reduction on the data taken at Pennsylvania State University's wind tunnel might also be beneficial.

### Acknowledgements

We would like to thank Bernardo Oliveira Vieira and Aman-deep Premi for assisting in the wind tunnel testing at The Pennsylvania State University. Special thanks go to Craig Rieker, a technician at the Icing Research Tunnel, NASA Glenn, who played an instrumental role in mentoring EAP through the manufacturing of the wake rake.

### References

- [1] Fred Thomas. *Fundamentals of Sailplane Design*. College Park Press, Silver Spring, Maryland USA, 1999. pp. 14–23.
- [2] K. H. Horstmann and A. Quast. Widerstandsverminderung durch Blasturbulatoren. Forschungsbericht DFVLR-FB 81-83, DFVLR Braunschweig Institut für Entwurfsaerodynamik, Braunschweig, Germany, 1981.
- [3] H. Schlichting. *Boundary Layer Theory*. McGraw Hill, 4th edition, 1960.
- [4] G. Bramesfeld. Untersuchung von laminaren Ablöseblasen am momentenarmen Laminarprofilen am Beispiel SB 13. Studientarbeit Nr. 96/2, Deutsche Forschungsanstalt für Luft- und Raumfahrt, Braunschweig, Germany, 1996.
- [5] A. Silverstein and S. Katzoff. A simplified method for determining wing profile drag in flight. *Journal of the Aeronautical Sciences*, 7(7), May 1940.
- [6] R. Johnson. At last: An instrument that reads drag! *Soaring*, 47(10), October 1983.
- [7] D. Althaus. An instrument for drag measurement in flight — optimization of flap settings. *Technical Soaring*, 19(1), January 1995.
- [8] L. Popelka, M. Matejka, D. Simurda, and N. Souckova. Boundary layer transition, separation and flow control on airfoils, wings and bodies in CFD, wind-tunnel and in-flight studies. *Technical Soaring*, 35(5):108–115, October–December 2011.
- [9] C. Plaisance. The development of an integrating wake rake for in-flight measurements of profile drag. Master's thesis, Department of Aerospace Engineering, Pennsylvania State University, University Park, Pennsylvania USA, 1997.
- [10] C. M. Brophy. Turbulence management and flow qualification of the Pennsylvania State University low turbulence, low speed, closed circuit wind tunnel. Master's thesis, Department of Aerospace Engineering, Pennsylvania State University, University Park, Pennsylvania USA, 1993.
- [11] R. Medina. Validation of the Pennsylvania State University low-speed, low-turbulence wind tunnel using measurements of the S805 airfoil. Master's thesis, Department of Aerospace Engineering, Pennsylvania State University, University Park, Pennsylvania USA, 1994.
- [12] D. M. Somers. Design and experimental results for the S805 airfoil. Report SR-440-6917, National Renewable Energy Lab, Golden, Colorado USA, October 1988.